Okamoto, A.; Horie, K.; Mita, I. *J. Am. Chem. Soc.* **1982**, *104*, 4469.
(2) (a) Zachariasse, K. A.; Duveneck, G.; Busse, R. *J. Am. Chem. Soc.* **1984**, *106*, 1045. (b) Zachariasse, K. A.; Duveneck, G.; Kuehnle, W. *Chem. Phys. Lett.* **1985**, *113*, 337. (c) Zachariasse, K. A.; Busse, R.; Duveneck, G.; Kuehnle, W. *J. Photochem.* **1985**, *28*, 237.
(3) Snare, M. J.; Thistlethwaite, P. J.; Ghiggino, K. P. *J. Am. Chem. Soc.* **1983**, *105*, 3328.
(4) (a) Bokobza, L.; Jasse, B.; Monnerie, L. *Eur. Polym. J.* **1977**, *13*, 921. (b) Bokobza, L.; Jasse, B.; Monnerie, L. *Eur. Polym. J.* **1980**, *16*, 715. (c) De Schryver, F. C.; Moens, L.; Van der Auweraer, M.; Boens, N.; Monnerie, L.; Bokobza, L. *Macromolecules* **1982**, *15*, 64.
(5) Ito, S.; Yamamoto, M.; Nishijima, Y. *Bull. Chem. Soc. Jpn.* **1981**, *54*, 35.
(6) (a) De Schryver, F. C.; Vandendriessche, J.; Toppet, S.; Demeyer, K.; Boens, N. *Macromolecules* **1982**, *15*, 406. (b) Evers, F.; Kobs, K.; Memming, R.; Tirrell, D. R. *J. Am. Chem. Soc.* **1983**, *105*, 5988. (c) Vandendriessche, J.; Palmans, P.; Toppet, S.; Boens, N.; De Schryver, F. C.; Masuhara, H. *J. Am. Chem. Soc.* **1984**, *106*, 3057.
(7) Collart, P.; Toppet, S.; Shou, Q. F.; Boens, N.; De Schryver, F. C. *Macromolecules* **1985**, *18*, 1026.
(8) (a) De Schryver, F. C.; Demeyer, K.; Van der Auweraer, M.; Quanten, E. *Ann. N. Y. Acad. Sci.* **1981**, *366*, 93. (b) De Schryver, F. C.; Demeyer, K.; Toppet, S. *Macromolecules* **1983**, *16*, 89.
(9) (a) Masuhara, H.; Tanaka, J. A.; Mataga N.; De Schryver, F. C.; Collart, P. *Polym. J.* **1983**, *15*, 915. (b) Collart, P.; Domeyer, K.; Toppet, S.; De Schryver, F. C. *Macromolecules* **1983**, *16*, 1390.
(10) Goedeweeck, R.; De Schryver, F. C. *Photochem. Photobiol.* **1984**, *39*, 515.
(11) Itagaki, H.; Horie, K.; Mita, I.; Washio, M.; Tagawa, S.; Tabata, Y.; Sato, H.; Tanaka, Y. *Chem. Phys. Lett.* **1985**, *120*, 547.
(12) Mita, I.; Horie, K. In *Degradation and Stabilization of Polymers*; Jellinek, H. H. G., Ed.; Elsevier: Amsterdam, 1983.
(13) Kanaya, T.; Goshiki, K.; Yamamoto, M.; Nishijima, Y. *J. Am. Chem. Soc.* **1982**, *104*, 3580.
(14) (a) Winnik, M. A. In *Cyclic Polymers*; Semlyen, A., Ed.; Applied Science Publishers: London, 1985. (b) Winnik, M. A.; Redpath, A. E. C.; Paton, K.; Danhelka, *J. Polym.* **1984**, *25*, 91. (c) Winnik, M. A.; Sinclair, A. M.; Beinert, G. *Macromolecules* **1985**, *18*, 1518.
(15) Longworth, J. W.; Bovey, F. A. *Biopolymers* **1966**, *4*, 1115.
(16) Itagaki, H.; Horie, K.; Mita, I.; Washio, M.; Tagawa, S.; Tabata, Y. *J. Chem. Phys.* **1983**, *79*, 3996.
(17) Sato, H.; Saito, K.; Miyashita, K.; Tanaka, Y. *Makromol. Chem.* **1981**, *182*, 2259.
(18) (a) Tagawa, S.; Katsumura, Y.; Tabata, Y. *Chem. Phys. Lett.* **1979**, *64*, 258. (b) Kobayashi, H.; Ueda, T.; Kobayashi, T.; Tagawa, S.; Tabata, Y. *Nucl. Instrum. Methods* **1981**, *179*, 223.
(19) (a) Durbin, J.; Watson, G. S. *Biometrika* **1950**, *37*, 409. (b) Durbin, J.; Watson, G. S. *Biometrika* **1951**, *38*, 159.
(20) (a) Birks, J. B. *Photophysics of Aromatic Molecules*; Wiley-Interscience: New York, 1970. (b) Birks, J. B.; Dyson, D. J.; Munro, I. H. *Proc. R. Soc. London, Ser. A* **1963**, *275*, 575.
(21) (a) Klöpffer, W. In *Organic Molecular Photophysics*; Birks, J. B., Ed.; Wiley: New York, 1973. (b) Klöpffer, W.; Liptay, W. *Z. Naturforsch., A* **1970**, *25A*, 1091.
(22) (a) Harrah, L. A. *J. Chem. Phys.* **1972**, *56*, 385. (b) Frank, C. W.; Harrah, L. A. *J. Chem. Phys.* **1974**, *61*, 1526. (c) Fox, R. B.; Price, T. R.; Cozzens, R. F.; McDonald J. R. *J. Chem. Phys.* **1972**, *57*, 534.
(23) (a) Bovey, F. A.; Hood, F. P.; Anderson, E. W.; Snyder, L. C. *J. Chem. Phys.* **1965**, *42*, 3900. (b) Williams, A. D.; Brauman, J. I.; Nelson, N. J.; Flory, P. J. *J. Am. Chem. Soc.* **1967**, *89*, 4807. (c) Williams, A. D.; Flory, P. J. *J. Am. Chem. Soc.* **1969**, *91*, 3111. (d) Pivcova, H.; Kolinsky, M.; Lim, D.; Schneider, B. *J. Polym. Sci., Part C* **1969**, *22*, 1093. (e) Bovey, F. A. *High Resolution NMR of Macromolecules*; Academic: New York, 1972.
(24) (a) Gorin, S.; Monnerie, L. *J. Chim. Phys.* **1970**, *67*, 869. (b) Stegen, G. E.; Boyd, R. H. *Polym. Prepr. (Am. Chem. Soc.—Div. Polym. Chem.)* **1978**, *19*, 595.
(25) Koda, S.; Nomura, H.; Niyahara, Y. *Bull. Chem. Soc. Jpn.* **1979**, *52*, 1828.
(26) Froelich, B.; Noel, C.; Jasse, B.; Monnerie, L. *Chem. Phys. Lett.* **1976**, *44*, 159.
(27) Tanabe, Y. *J. Polym. Sci., Polym. Phys. Ed.* **1985**, *23*, 601.
(28) These values are calculated by Koda et al.[25] by extrapolating the data obtained by Monnerie et al.[26] to room temperature.
(29) Blonski, S.; Sienicki, K.; Herman, A. *Macromolecules* **1987**, *20*, 329.

Role of Symmetry in the Formation of *n*-Paraffin Solid Solutions

Douglas L. Dorset

Electron Diffraction Department, Medical Foundation of Buffalo, Inc., Buffalo, New York 14203. *Received April 3, 1987*

ABSTRACT: Single-crystal electron diffraction patterns from epitaxially crystallized binary solids of *n*-$C_{32}H_{66}$/*n*-$C_{36}H_{74}$ and *n*-$C_{33}H_{68}$/*n*-$C_{36}H_{74}$ have been reanalyzed to determine the symmetry rules for solid solution formation. For these orthorhombic structures, the symmetry alternates sequentially between the $Pca2_1$ space group of the even-chain structure and the $A2_1am$ space group (or possibly twinned Aa) of the odd-chain structure with increasing concentration of the longer chain component, irrespective of whether the solid is comprised of even–even or odd–even chain combinations. Similar structural features are found for a commercial multicomponent paraffin wax. The sequence of lamellar spacings is regulated by archetypical crystal packing(s) for any concentration region so that, in the microcrystalline state, increase in lamellar thickness is steplike and not a smooth function like Vegard's law. In this sense, the solid solutions are not continuous, even when the chain length difference is small and the pure components have the same crystal structure.

Introduction

Because of its importance for understanding the physical behavior of various polydisperse linear chain molecules (e.g., lipids, polymers), the solid solubility of binary *n*-paraffin aggregates has been an object of continued interest for at least 60 years. With an overview of calorimetric and diffraction data as reviewed by Mnyukh,[1] Kitaigorodskii formulated rather strict rules for the formation of continuous solid solutions. The first rule states that the molecular size difference (which can be inversely stated as a parameter of geometrical similarity[2]) cannot be too large.[2,3] Expression of this rule is verified by the characteristics of phase diagrams in Mnyukh's review; hence, if the paraffin chain lengths are too different, a eutectic is formed. The upper limit for length difference permitted for solid solution formation is discussed by several authors.[4,5]

The second rule considers molecular and/or crystal symmetry. According to Kitaigorodskii, if the molecules are not asymmetric (as in the case of linear paraffins), then the addition of solute A to crystal solvent B must not raise the symmetry of B. Addition will either lower the symmetry of B or leave its symmetry unchanged. For this reason, proposed solid solubility of even- with odd-chain

0024-9297/87/2220-2782$01.50/0

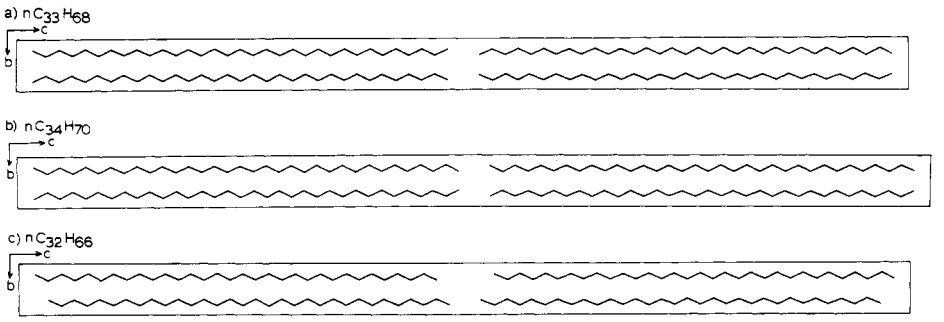

Figure 1. Crystal structures of *n*-paraffins ((100) projection): (a) High-temperature B-form of odd-chain paraffins (n-$C_{33}H_{68}$). Space group either $A2_1am$[8] or Aa;[20] the former utilizes the mirror symmetry of the chains; $a = 7.52$, $b = 4.98$, $c \simeq 2.546n + 3.75$ Å, where n is the number of chain carbons.[18] (The unit cell repeat is similar to the lower temperature A-form.) (b) Orthorhombic form of even-chain paraffins (n-$C_{34}H_{70}$). Space group $Pca2_1$;[15] $a = 7.44$, $b = 4.96$, $c = 2.540n + 3.693$ Å, where n is again the number of carbon atoms.[18] (c) How to obtain an odd-chain paraffin packing from even chains. Alternating chains in the structure of n-$C_{32}H_{66}$ (homologous to (b)) are translated one methylene unit and rotated 180° around the long axis. The resulting structure places end methyl groups with the same polarity in (a) but with half occupancy of these sites. Such a structure was first suggested by Lüth et al.[8]

alkanes in the literature was stated by Kitaigorodskii to be impossible on grounds of different crystal symmetries.[3,6]

A major problem in the study of *n*-paraffin solid solutions is that the effects of symmetry change can be very subtle. If two paraffins, e.g., an odd and even, with both packing with orthorhombic monolamellar layers, both have the same methylene subcell, then the only observable differences are in the packing of the end planes of adjacent lamellae as depicted in Figure 1. Mnyukh[1] has stated how such subtle differences can remain undetected in calorimetric measurements, perhaps leading to a misinterpretation of a phase diagram. Diffraction data are useful for clarifying the structural significance of the phase diagram, but use of Debye–Scherrer powder patterns from polycrystalline arrays also makes the identification of small symmetry changes quite difficult. To our knowledge there have been only two single-crystal X-ray studies of *n*-paraffin solid solutions,[7,8] owing to the great difficulty in sample preparation. Recently, this difficulty has been largely overcome in our laboratory with the use of epitaxially crystallized microcrystals of binary solids for electron diffraction structure analysis. With this technique we have used single-crystal diffraction patterns from a projection onto the chain axis to demonstrate the formation of solid solutions[9] and/or eutectic mixtures,[10] and even to determine the crystal structure of one solid solution. The measured variation of *average* lamellar spacing with increasing concentration of larger component[9] also was entirely consistent with those determined in earlier X-ray studies,[1] and the relative chain length differences leading to fractionation[10] also agreed with earlier observation.[1,4,5]

An unexpected result from our earlier study is that, within the limiting molecular chain difference, continuous solid solutions seemed to be permitted for the higher energy quasi-orthorhombic polymorph of an odd-chain paraffin n-$C_{33}H_{68}$ with the orthorhombic polymorph of an even-chain paraffin n-$C_{36}H_{74}$,[9] despite Kitaigorodskii's prediction that they should fractionate. A more striking violation of his theorems is found in the X-ray study[8] of two shorter even-chain *n*-paraffins where the pure components have the same triclinic crystal structure but the intermediate solid solutions pack in a *higher* symmetry orthorhombic cell. Because the reasons for this discrepancy are not clearly defined, this paper investigates this symmetry problem in greater detail than in our earlier publications which dealt mainly with the mutual molecular size constraints to cosolubility.

Materials and Methods

Sample Preparation. Solid solutions of *n*-paraffins, i.e., n-$C_{32}H_{68}$ or n-$C_{33}H_{68}$, with n-$C_{36}H_{74}$, were the same as those prepared 2 years ago, as reported in our earlier paper.[9] Briefly, the solid solutions were epitaxially crystallized on benzoic acid following the methodology described by Wittmann et al.[11] Since these solutions have aged, it was also thought that relaxation effects (e.g., translational shift, straightening of chain kinks) might be noted in the electron diffraction data. A commercially available *n*-paraffin solid solution, i.e. Gulfwax from the Gulf Oil Corporation (Houston, TX), was also epitaxially crystallized on benzoic acid for comparison to studies of our binary solids. The peak melting temperature of this solid solution determined by DSC (Mettler FP800) is 53.8 °C, compared to 55.5–56.1 °C reported earlier.[12]

Electron Diffraction. Selected area electron diffraction patterns obtained at 100 kV with a JEOL JEM-100B electron microscope were recorded on Kodak DEF-5 X-ray film. As usual, precautions were taken to minimize radiation damage of the specimens.[13] The camera length is calibrated with a gold Debye–Scherrer diagram. Measurements of interpeak spacings on electron diffraction patterns were made with a film reading device for precession X-ray films manufactured by Charles Supper, Inc.

Computations. The major feature of $0kl$ electron diffraction patterns used in this paper are the indices of the most intense $00l$ and $01l$ reflections. Although the two rectangular crystal structure projections considered here (Figure 1) have different symmetry (i.e. odd-chain structure, plane group cm with $k + l = 2g$; even-chain structure, plane group formally pm but $l = 2g$ due to a glide plane $\perp a$), their $0kl$ diffraction patterns have similar index rules for identification of the seemingly predominant structural component in the solid solution (or monodisperse crystal). Hence, as verified with model structure factor calculations on the known crystal structures of odd[8,14] and even[15] *n*-paraffins using Doyle–Turner electron scattering factors,[16] the $00l$ intensities have even index in either case so that the most intense reflections at high angle for any paraffin C_nH_{2n+2} occur at $l = 2n + 2$ and $2n + 4$. The $01l$ reflections have odd or even indices depending on whether the structures resemble respectively an odd or even *n*-paraffin, but, for both examples, indices of the most intense reflections correspond to $l = n$ and $l = n + 2$. This is illustrated schematically in Figure 2.

Results

Binary Solid: n-$C_{32}H_{66}$/n-$C_{36}H_{74}$ (Even–Even). Indices of reflections in $0kl$ electron diffraction patterns from n-$C_{32}H_{66}$/n-$C_{36}H_{74}$ binary solids immediately indicate that the diffraction pattern symmetry of the pure components is not preserved over all mole fractions of the binary solids (Figure 3). Rather it appears that a paraffin crystal structure with limiting lamellar length dominates the structure of a given composition domain. As more and more long-chain component is present in the binary solid, the symmetry sequentially alternates between even and odd paraffin unit cell packings until, at higher mole fractions of n-$C_{36}H_{74}$, only the longest chain packing is found. There are intermediate concentration ranges where

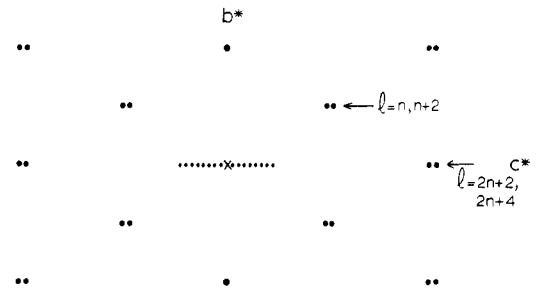

Figure 2. Representative $0kl$ diffraction patterns from an n-paraffin crystal structure. For odd-chain structure the observed reflections occur at $k + l = 2g$; for even-chain structures these occur at $l = 2g$ (here g is an integer). In either case intense reflections occur at $l = n, n + 2$ for the $01l$ row and at $l = 2n + 2, 2n + 4$ for the $00l$ row, permitting identification of a pure paraffin C_nH_{2n+2} from the indexing of the pattern.

two or more preferred crystal structures might be found. In samples that were freshly crystallized from the melt (Figure 3a), these overlapping areas may be more extensive than for aged samples (Figure 3b).

As found before[9] the average lamellar spacing for binary solids lies above the Vegard's law line (Figure 4a). (Here we assume that increase of this spacing accounts for most of the volume change of the structure, as accepted by other workers,[1] even though minor changes in the lateral spacings were found in some recent work.[17]) On the other hand, the averaged lamellar spacings for any paraffin packing type correspond very closely to the spacing of the pure component[18] (Figure 5a), irrespective of the formal composition of any binary solid. Hence the intermediate lamellar spacing values in Figure 4a express the averaged presence of two or more crystal structures for a microcrystalline array, where each separate microcrystal has its own crystal structure. Thus, for any single microcrystal of a binary solid solution, the electron diffraction pattern seems to originate from a pure paraffin, both in terms of lamellar spacing and symmetry. The only difference lies in the resolution of the inner $00l$ row.

Although the resolution of inner-order $00l$ reflections is also a function of composition, where only microcrystals of either composition extreme seem to pack with a minimum of chain-end voids (see below), there is no convincing evidence for an increased resolution of individual solid solution on aging (Figure 6a), which could be caused by the unfolding of chain kink defects to minimize the number and size of chain-end voids. Nevertheless significant resolution differences can be seen for a particular chain combination (Figure 7a,b), although these differences also do not correspond to any particular crystal structure when two or more are favored for a given concentration region.

Binary Solid: n-$C_{33}H_{68}$/n-$C_{36}H_{74}$ (Odd–Even). The results from the odd–even binary solids are quite similar to those of the even–even system presented above. In terms of indexed diffraction patterns, the overlap of possible crystal structures seems to occupy larger concentration ranges than found for the even–even system. Again the apparent crystal structures alternate as odd, even, odd, even, as one progresses from pure n-$C_{33}H_{68}$ to pure n-$C_{36}H_{74}$ (Figure 3c,d).

The average lamellar spacings for particular binary compositions again fall above the Vegard's law line (Figure 4b). Averaged lamellar spacings within a certain crystal structure type (irrespective of concentration), however, are close to their theoretical values[18] (Figure 5). The lamellar diffraction resolution for intermediate chain combinations is again less than that of the pure components (Figure 6b), in agreement with the above findings for even–even binary solids. Again there is no clear evidence for improved $00l$ diffraction resolution after the samples have aged for 2 years.

Commercial Solid Solution (Gulfwax). Although the commercial paraffin wax is a multicomponent solid, described as a blend of n-paraffins from n-$C_{26}H_{56}$ to n-$C_{30}H_{62}$,[12] the single-crystal $0kl$ electron diffraction patterns are very similar in appearance (Figure 7c) to those of binary solid solutions, because the inner lamellar $00l$ reflections have attenuated resolution. Indices of these patterns indicate that the blend mostly crystallizes as the crystal structure of n-$C_{29}H_{60}$, although occassionally patterns which are indexed as the even-chain paraffins, n-$C_{28}H_{58}$ and n-$C_{30}H_{62}$, are also found. The average chain length is somewhat shorter than the n-$C_{31}H_{64}$ equivalent found in the earlier X-ray study[12] and probably accounts for the observed difference in melting points. Average lamellar spacings within a paraffin species (as determined

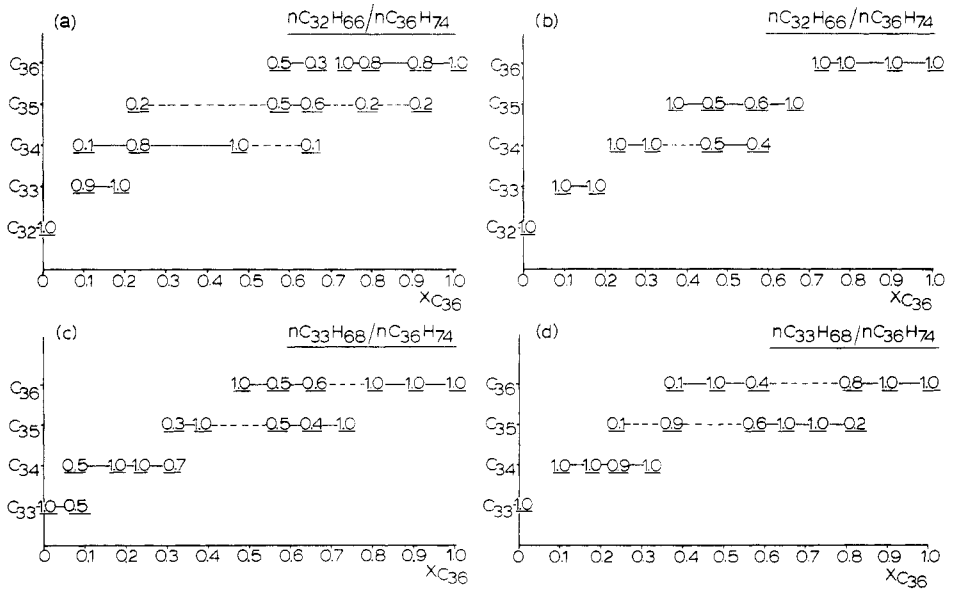

Figure 3. Indices of electron diffraction patterns as in Figure 2 for different mole fractions of binary solids indicate that the structure of the unit cell resembles the paraffin C_nH_{2n+2}. The numbers indicate the fraction of an experimental selection which conforms to one crystal structure or another: (a) n-$C_{32}H_{66}$/n-$C_{36}H_{74}$ just grown on benzoic acid; (b) same as (a) but aged for 2 years; (c) n-$C_{33}H_{68}$/n-$C_{36}H_{74}$ just grown on benzoic acid; (d) as in (c) but aged for 2 years.

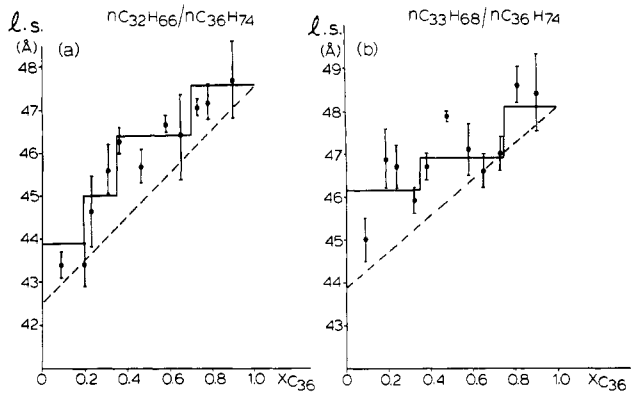

Figure 4. Relationship between lamellar spacing versus mole fraction for aged binary solids. The dotted line is the linear expansion predicted by Vegard's law since the lamellar spacing increase accounts for most of the volume changes.[1] The step function is drawn from the largest chain length crystal structure (as determined by diffraction pattern index) which dominates concentration domains in the binary solid series. Experimental points are average lamellar spacings for particular mole fractions with standard deviations. (a) n-$C_{32}H_{66}$/n-$C_{36}H_{74}$; (b) n-$C_{33}H_{66}$/n-$C_{36}H_{74}$. (Note that the positions of the pure lamellar spacings were increased slightly to represent the somewhat larger average experimental values found for this latter series as indicated in Figure 5. This may be due to a slight calibration error for the odd–even series of binary solids or may be consistent with earlier observations of electron diffraction lamellar spacings from pure paraffins,[9,14] which are sometimes slightly larger than X-ray diffraction values.

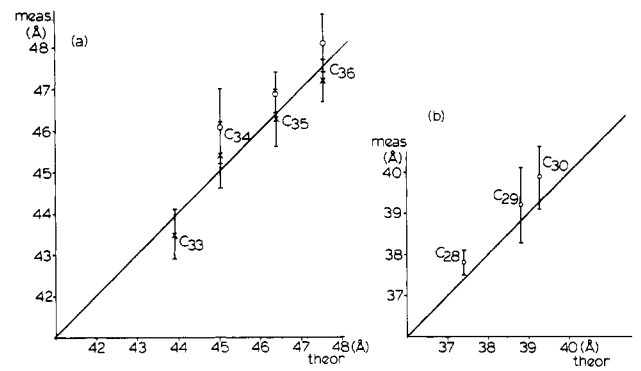

Figure 5. (a) Plot of averaged lamellar spacings within one crystal structure type (as indicated by the indexed diffraction pattern) versus the theoretical value for the pure paraffins.[18] These averages are made irrespective of the mole fraction of the binary solid; i.e., if the index of a pattern for a sample from $X_{C36} = 0.56$ indicates that the paraffin resembles n-$C_{36}H_{74}$ this lamellar value is averaged with that from another pattern indicating the same structure, e.g., at $X_{C36} = 0.90$, etc. The average values for the n-$C_{32}H_{66}$/n-$C_{36}H_{74}$ binary solids (×) with standard deviations; those for the n-$C_{33}H_{68}$/n-$C_{36}H_{74}$ series (○). The line is that of perfect correlation. (b) Averages of lamellar spacings representing n-paraffin structures indicated by $0kl$ diffraction pattern indices for epitaxial crystals of the multicomponent Gulfwax.

by index of $0kl$ reflections) are shown in Figure 5b to be very close to their theoretical values.[18]

Discussion

The advantages of electron diffraction measurements on individual microcrystals over powder X-ray diffraction measurements of a bulk sample are clearly shown by the data presented in this paper. The smooth increase of lamellar spacing upon addition of longer chain component to a binary solid indicated by powder X-ray measurements leads to a false view of the structural changes in the mixed-chain crystalline lattice and tempts the experimentalist to explain his data in terms of Vegard's law or

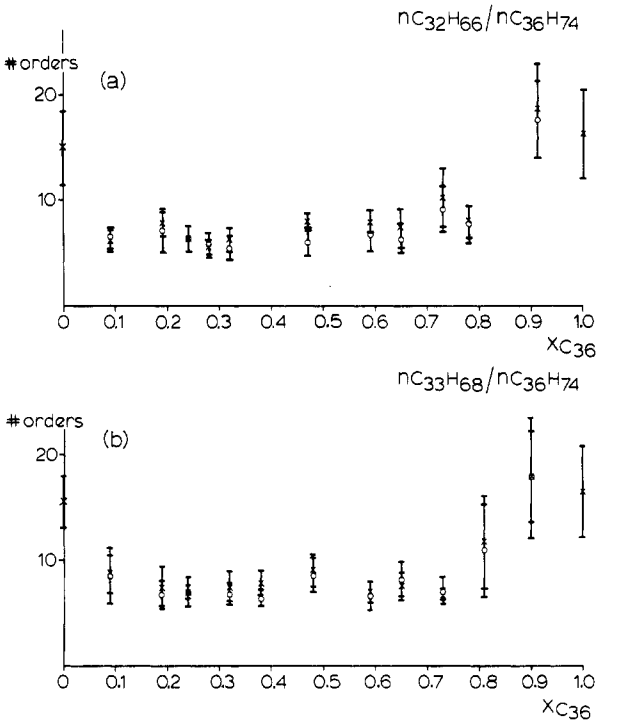

Figure 6. Experimentally measured lamellar diffraction resolutions for binary solid solutions either just crystallized on benzoic acid (○) or aged for 2 years (×): (a) n-$C_{32}H_{66}$/n-$C_{36}H_{74}$; (b) n-$C_{33}H_{68}$/n-$C_{36}H_{74}$. The slight resolution increase for most aged samples does not appear to be statistically significant—nor is there any dependence of diffraction resolution on any particular crystal structure (Figure 3) when more than one is possible for any concentration.

a revised version of this law which accounts only for the dominance of the longer chain crystal structure at large concentrations of higher molecular weight component.[1] It is now seen that the smooth increase of lamellar spacing is merely a weighted average of several lamellar spacings, which in the diffraction pattern of a bulk sample would give a Gaussian spread to the lamellar spots. This spread may not be detected because of the angular spread of diffraction intensity due to textural distributions etc.

From the data presented above, it is clear that when a particular binary paraffin solid crystallizes as a given n-paraffin crystal structure, the symmetry and intensity distribution of the diffraction pattern, as well as the measured lamellar spacing, corresponds very closely to the values for a pure paraffin. The progression of crystal packings with increasing concentration of larger chain length component sequentially adopts the next longest pure paraffin crystal structure, irrespective of whether that paraffin is even or odd. Thus, instead of Vegard's law, the rule for binary solid lamellar spacing with changing concentration is a step function as illustrated in Figure 4. As shown in Figure 3, there are concentration regions where either of two crystal structures can be assumed by the chain aggregate. These rules also appear to be true for a multicomponent system. Thus, in terms of Kitaigorodskii's criteria[3] for a continuous paraffin solid solution, such continuity simply does not exist!

This behavior is probably explainable in terms of lattice energy. Although the symmetries of the two crystal structures in Figure 1 are different, it is clear that their differences are expressed only by the symmetry relationship between otherwise identical chain-end packings and not the polymethylene subcell. This is also why such structural discontinuities are not easily detected by calorimetric determination of phase diagrams. (It will be of

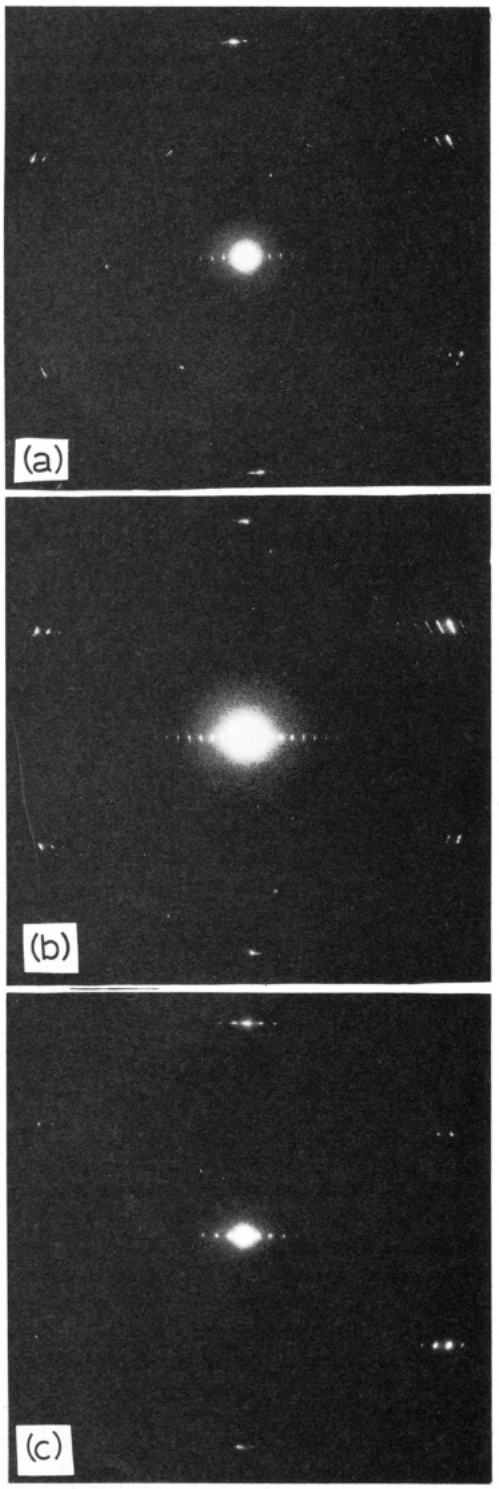

Figure 7. Experimental electron diffraction patterns from binary solids (a), (b) n-$C_{32}H_{66}$/n-$C_{36}H_{74}$, $X_{C36} = 0.47$. Note differences in resolution for the same composition lending to the standard deviation in Figure 6; (c) $0kl$ pattern from the Gulfwax sample.

interest to investigate the difference in packing energy for the two crystal forms by accurate potential function calculations.[19])

It remains to be shown how arbitrary n-paraffin mixtures can assume a crystal structure characteristic of either odd or even pure components. In comparing the two rectangular projections in Figure 1a,b one finds that the average direction of chain-end methyl groups can be changed by a rotation around one chain axis and translation by one methylene group as in Figure 1c. (Such chain rotations have been found experimentally in the solid–solid

Table I
Comparison of Electron Diffraction Structure Factor Magnitudes from n-$C_{33}H_{68}$ (B-Form, I) and the Disordered n-$C_{32}H_{66}$ Structure (II) Which Resembles n-$C_{33}H_{68}$ (See Figure 1)

$0kl$	$\|F\|_I$	$\|F\|_{II}$	$0kl$	$\|F\|_I$	$\|F\|_{II}$
0,0,2	0.21	0.35	0,0,66	0.12	0.11
0,0,4	0.21	0.33	0,0,68	0.36	0.36
0,0,6	0.20	0.31	0,0,70	0.27	0.27
0,0,8	0.19	0.28	0,1,29	0.10	0.10
0,0,10	0.18	0.24	0,1,31	0.14	0.14
0,0,12	0.18	0.21	0,1,33	0.28	0.29
0,0,14	0.18	0.18	0,1,35	0.60	0.59
0,0,16	0.16	0.13	0,1,37	0.11	0.09
0,0,18	0.14	0.09	0,2,0	1.60	1.55
0,0,20	0.12	0.06	0,2,68	0.17	0.11
0,0,22	0.12	0.04	0,2,70	0.13	0.13
0,0,24	0.12	0.03	0,3,33	0.22	0.23
0,0,26	0.11	0.02	0,3,35	0.50	0.49

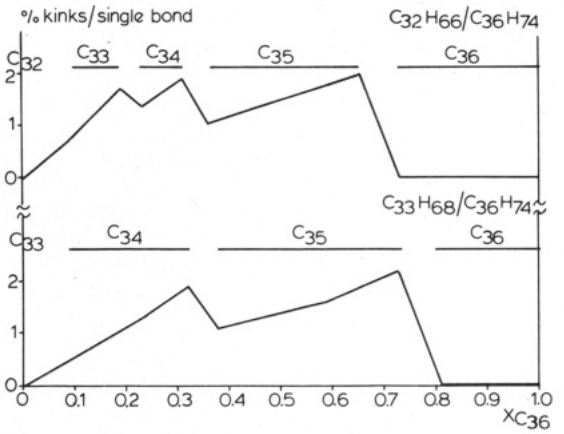

Figure 8. Minimal kink populations for structures suggested by Figure 3b,d for the two respective binary solid series. In the calculations, enough kinks q were included into the longest chain component to make it conform to the crystal structure of the largest average paraffin which dominates a concentration domain. This number q was divided by 33 to provide the average over the internal bonds of a $C_{36}H_{74}$ chain and is multiplied by the mole fraction of this longer chain component to give a kink concentration per bond in the indicated crystal structure. A limit of 2% is approached before transition to a new crystal structure.

transition of odd-chain paraffins.[20]) This changes the average crystal structure from one where the average chain has a center of symmetry to one where it has a reflection plane perpendicular to the chain and intersecting the chain center. (A similar process will make an pseudo-even-chain crystal structure from a binary solid made up predominately of odd chains.) In this crystal structure, the occupancy of chain end carbons will therefore be 0.50 for a 1:1 binary solid so that there is an average void of one carbon for every other methyl group. Structure factor calculations based on this model, e.g., for a pseudo-n-$C_{33}H_{68}$ structure formed from n-C_{32} chains (Figure 1c), indicate that the $0kl$ intensity distribution is very similar to that of the pure paraffin (Table I); the major difference is seen in the slight attenuation of $(00l)$ resolution (Figure 7) due to the void content.[9,31] This structural model is identical with one proposed by Lüth et al.[8] in their crystal structure analysis of n-$C_{20}H_{24}$/n-$C_{22}H_{46}$ where the mixed-chain solids assumed an orthorhombic structure unlike the triclinic polymorph of the pure components. The space group identified by them (using our unit cell axis designation) is $A2_1am$ instead of the monoclinic Aa assigned by Piesczek et al.[20] As noted above, the higher symmetry of this solid solution also violates Kitaigorodskii's symmetry rules. (Our crystal structure analysis of the higher energy form

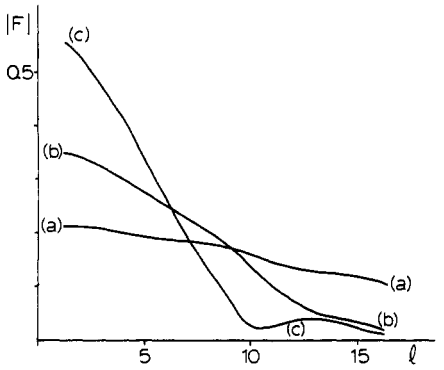

Figure 9. Plot of low-angle 00l structure factor magnitudes for various structures similar to the n-$C_{33}H_{68}$ crystal structure of (a) pure n-$C_{33}H_{68}$ as in Figure 1a; (b) model structure in Figure 1c made up of two n-$C_{32}H_{68}$ chains and resulting in an occupancy of 0.5 at the end carbon of the n-$C_{33}H_{68}$ crystal structure; (c) as in (b) except that the end carbons have populations 0.125 for C_1, C_1' and 0.625 for C_2,C_2 (where these designate the terminal carbons of the chain). This would simulate the presence of larger chain end voids caused, for example, by an increased populations of chain kink defects.

of n-$C_{33}H_{68}$[14] also does not exclude this space group assignment since we did not observe the twinning claimed in the earlier X-ray study.[20])

The advantages of this crystal packing becomes clear. Mutual translation of two short chains produces a longer unit cell to accommodate a longer chain component. It is also apparent that there must be some additional shortening of the longer chain for inclusion into the unit cell. Such shortening can be accomplished by "kinks" (i.e., gauche-trans-gauche^{-1} conformers) along the chain since each kink defect will retract a carbon chain by approximately one methylene repeat, as illustrated in an earlier study of chain melting.[21] (Although the kink models used in these studies are based on known X-ray crystal structures, an extensive treatment of polyethylene chain deformations is found in a paper by Reneker and Mazur.[22]) If, for example, these kinks are distributed equally over 33 C–C bonds for a $C_{36}H_{74}$ chain (excluding the two end bonds), then, as shown in Figure 8, the average defect population per bond is only slightly higher than the 0.5% detectability claimed for infrared spectroscopic measurements.[23] For the binary structures considered here, it is interesting to note that as the requisite kink population per C–C bond would approach, e.g., 2%, then the packing is seen to transform to the next longer chain crystal structure.

There is no question that chain kinks are present in the paraffin crystal structures, even for pure materials—e.g., as evidenced by the strong continuous diffuse scatter in electron diffraction patterns from paraffins held at 16 K.[23] Samples crystallized from the melt will contain a number of metastable kink sites, as revealed by the limited resolution of the pattern in Figure 6a. As shown earlier,[9,21,25,26] kinks enlarge the chain-end voids in the average structure beyond the minimum value needed to accommodate the longer chain component in the binary solid, so that the population densities of terminal carbon positions on either end of the chain have an approximately Gaussian distribution and thus these intensities are limited in resolution (Figures 6 and 9). As the chain kinks unfold and the chain-end voids become smaller the resolution of these data could improve, but our data do not indicate a marked relaxation of this type over 2 years. Thus there are at least two mechanisms, chain translation and kinking, which combine to accommodate two different chain lengths in a single average crystal packing. The limiting factor here, as evidenced also by our study of fractionated paraffin mixtures, appears to be the size of the chain-end voids and their effect on the lattice energy.

The model presented here also is not inconsistent with earlier spectroscopic studies on shorter chain paraffin binary solids,[23] which apparently are not long enough to retain many kink defects in the crystal lattice.[26] Although the number of internal chain kinks was found in the earlier study[23] to be very low for equilibrated samples, the number of kinks proposed in this study just to accommodate a longer chain into a smaller chain crystal structure is small enough not to be easily detected. Moreover, the large number of chain-end kinks actually observed in the spectroscopic study at low concentrations of the longer chain component[23] could also be important here, not only for shortening the chain but also for establishing the correct average symmetry needed for the longer component in the end plane region.

Summary

Because a number of aspects of chain packing are considered here, it is useful to summarize the findings of this study of binary paraffin solids:

(1) In terms of the symmetry rules given by Kitaigorodskii there is no continuity of paraffin solid solutions even for solids where the two components have an adequately small chain length difference—and not even when the pure components pack in the same crystal structure.

(2) Although the unit cell volume increases linearly with lamellar spacing, the sequence of binary paraffin solids does not obey Vegard's law. The binary solid for any concentration range is characterized by limiting paraffin crystal structure (or two or more of them) which determines the maximum lamellar spacing(s) and the symmetry for individual polydisperse microcrystals. This leads to a step-function model for chain length which gives a better account of experimental data.

(3) Although a minimal number of chain kinks is required to stabilize a binary solid crystal structure, an additional number may be present in longer chain paraffin solid solutions as evidenced by the limited resolution of (00l) reflections for intermediate concentrations.

Acknowledgment. I am grateful for research support for this work from the National Science Foundation (DMR86-10783).

References and Notes

(1) Mnyukh, Yu. V. *Zh. Strukt. Khim.* **1960**, *1*, 370.
(2) Kitaigorodskii, A. I. *Mixed Crystals*; Springer: Berlin, 1984; 219.
(3) Kitaigorodskii, A. I. *Organic Chemical Crystallography*; Consultants Bureau: New York, 1961; p 231 ff.
(4) Asbach, G. I.; Kilian, H.-G.; Stracke, Fr. *Colloid Polym. Sci.* **1982**, *260*, 151.
(5) Matheson, R. R., Jr.; Smith, P. *Polymer.* **1985**, *26*, 288.
(6) Kitaigorodskii, A. I. *Molecular Crystals and Molecules*; Academic: New York, 1983; p 116 ff.
(7) Smith, A. E. *Acta Crystallogr.* **1957**, *10*, 802.
(8) Lüth, H.; Nyburg, S. C.; Robinson, P. M.; Scott, H. G. *Mol. Cryst. Liq. Cryst.* **1974**, *27*, 337.
(9) Dorset, D. L. *Macromolecules* **1985**, *18*, 2158.
(10) Dorset, D. L. *Macromolecules* **1986**, *19*, 2965.
(11) Wittmann, J. C.; Hodge, A. M.; Lotz, B. *J. Polym. Sci., Polym. Phys. Ed.* **1983**, *21*, 2495.
(12) Chichakli, M.; Jessen, F. W. *Ind. Eng. Chem.* **1967**, *59* (5), 86.
(13) Dorset, D. L. *J. Electron Microsc. Technol.* **1985**, *2*, 89.
(14) Dorset, D. L. *J. Polym. Sci., Polym. Phys. Ed.* **1986**, *24*, 79.
(15) Teare, P. W. *Acta Crystallogr.* **1959**, *12*, 294.
(16) Doyle, P. A.; Turner, P. S. *Acta Crystallogr., Sect. A.* **1968**, *A24*, 390.

(17) Retief, J. J.; Engel, D. W.; Boonstra, E. G. *J. Appl. Crystallogr.* **1985**, *18*, 156.
(18) Nyburg, S. C.; Potworowski, J. A. *Acta Crystallogr., Sect. B* **1973**, *B29*, 347.
(19) Lundager-Masden, H. E.; Boistelle, R. *Acta Crystallogr., Sect. A* **1976**, *A32*, 828.
(20) Piesczek, W.; Strobl, G. R.; Malzahn, K. *Acta Crystallogr., Sect. B* **1974**, *B30*, 1278.
(21) Dorset, D. L.; Moss, B.; Wittmann, J. C.; Lotz, B. *Proc. Natl. Acad. Sci. U.S.A.* **1984**, *81*, 1913.
(22) Reneker, D. H.; Mazur, *J. Polym.* **1983**, *24*, 1387.
(23) Maroncelli, M.; Strauss, H. L.; Snyder, R. G. *J. Phys. Chem.* **1985**, *89*, 5260.
(24) Dorset, D. L.; Moss, B.; Zemlin, F. *J. Macromol. Sci. Phys.* **1985–1986**, *B24*, 87.
(25) Asbach, G. I.; Geiger, K.; Wilke, W. *Colloid Polym. Sci.*, **1979**, *257*, 1049.
(26) Craievich, A. F.; Denicolo, I.; Doucet, J. *J. Phys. Rev. B. Condens Matter* **1984**, *30*, 4782.

Characterization of the Stereostructure of Three Poly(1-butenes): Discrimination between Intramolecular and Intermolecular Distributions of Defects in Stereoregularity

R. D. Icenogle* and G. B. Klingensmith

Shell Development Company, Westhollow Research Center, Houston, Texas 77001.
Received February 18, 1987

ABSTRACT: A very complete characterization of the stereostructure of three poly(1-butenes) was achieved by separating the polymers into components of increasing isotacticity with successive recrystallizations from hot *n*-heptane solutions and analyzing the components with ^{13}C nuclear magnetic resonance, gel permeation chromatography, and other techniques. The poly(1-butenes) analyzed were (1) a highly isotactic homopolymer prepared by using a conventional titanium chloride/alkylaluminum catalyst, (2) a moderately isotactic homopolymer prepared by using a variation of this conventional catalyst, and (3) a moderately isotactic homopolymer prepared by a high activity supported titanium chloride catalyst developed at Shell Development Co. It is shown that the two materials prepared by the conventional catalyst are predominantly mixtures of atactic molecules with highly isotactic molecules, while the material prepared by the high activity catalyst contains a large proportion of molecules of intermediate tacticity. The polymer of intermediate tacticity prepared by the conventional catalyst behaves like a plasticized thermoplastic, while the polymer of intermediate tacticity prepared by the supported catalyst shows more elastomeric properties.

Introduction

Polymerization of propylene, 1-butene, and higher α-olefins by Ziegler–Natta catalysts, which are combinations of a compound of a group IV–VIII (4–10)[22] transition metal with an organometallic compound of a group I–III (1, 2, 13) nontransition element, can produce polymers with a high degree of stereochemical regularity.[1] The most powerful experimental tool we have to determine the stereostructure of these polymers is ^{13}C nuclear magnetic resonance (NMR), which gives information about the stereochemical structure because the NMR chemical shifts of the carbon atoms are sensitive to the configuration of closely bonded neighbors.[2,3] Different measures characterizing the average degree of isotacticity of a polymer sample can be derived from the NMR spectrum of the whole polymer,[3] but to more completely determine the stereostructure of a polymer, it is useful to separate the polymer into components of varying isotacticity and then analyze each of these components. This gives information about the distribution of isotacticity among the polymer molecules, just as a separation on the basis of molecular weight gives information on the distribution of chain lengths among the polymer molecules.[4] Understanding the stereostructure of these polymers in detail is important in understanding the mechanism of olefin polymerization[5] and the relationship of these structures to the morphology and properties of the polymers.[6–10]

In this work three poly(1-butenes) were analyzed: (1) a highly isotactic homopolymer prepared by using a conventional titanium chloride/alkylaluminum catalyst, (2) a moderately isotactic homopolymer prepared by using a variation of this conventional catalyst, and (3) a moderately isotactic homopolymer prepared by a high activity supported titanium chloride catalyst developed at Shell Development Co. Each of these materials was separated into components varying in crystallizability by sequential crystallization from hot *n*-heptane solutions and isolation of the soluble and insoluble components. More specifically, an initial recrystallization of the whole material was followed by subsequent recrystallization of the soluble component, the insoluble component, or both, and this procedure was repeated until the desired degree of separation was obtained, the ratio of heptane to polymer being adjusted at each step of the separation. The resulting components were then analyzed by ^{13}C NMR, gel permeation chromatography (GPC), and other techniques. From this work a very complete characterization of the stereostructure of these materials was achieved, and it was found that the two materials prepared by the conventional catalysts were predominantly mixtures of atactic molecules with highly isotactic molecules, while the material prepared by the high activity catalyst contains a large proportion of molecules of intermediate tacticity. The physical properties of these materials reflect these structural differences.

Materials and Methods

Sample I is a commercial highly isotactic poly(1-butene) homopolymer manufactured by Shell Chemical Co. and made with a conventional titanium chloride/alkylaluminum catalyst. Sample II is a poly(1-butene) homopolymer of intermediate isotacticity made with the same conventional catalyst but without a selectivity control agent. Sample III is a poly(1-butene) homopolymer of

*Current address: Teknor Apex Co., Pawtucket, RI 02861-0290.

0024-9297/87/2220-2788$01.50/0